Charmonium sum rules applied to a holographic model

Paul M. Hohler

Charmonium sum rules applied to a holographic model

Paul M. Hohler*

Department of Physics, University of Illinois, Chicago, Illinois 60607-7059, USA

The heavy quark QCD sum rules are applied to a model of charmonium based upon the gauge/gravity duality. We find that there is strong agreement between the moments of the polarization function calculated from the holographic model and the experimental data suggesting that the model is consistent with the heavy quark QCD sum rules at zero temperature.

I. INTRODUCTION

A new model of charmonium in the context of the gauge/gravity duality was constructed at zero temperature using spectral data so that the model exactly reproduced the masses and decay constants of the ground state, J/ψ, and the first excited state, ψ' [1]. This model was then considered at finite temperature, where the dissociation temperature of charmonium was investigated. In this paper, we will examine the zero temperature model in the context of heavy quark QCD sum rules [2–4]. As a reference point, the results will be compared with a similar analysis of a different holographic model of charmonium [5, 6].

QCD sum rules were first developed by Shifman, Vainshtein, and Zakharov (SVZ) [2, 3]. They provide a systematic way to compare theory and experiment and have been used in a wide variety of systems. QCD sum rules are based upon the two-point vector-vector correlation function of the heavy quark (charm) current; at zero temperature this correlation function can be expressed in terms of one function, the polarization function, $\Pi^{(c)}(Q^2)$,

$$\int d^4x\, e^{iqx}\, \langle J_\mu(x) J_\nu(0) \rangle = (q_\mu q_\nu - q^2 g_{\mu\nu})\, \Pi^{(c)}(Q^2), \quad (1)$$

where the charm current is defined as, $J^\mu = \bar{c}\gamma^\mu c$, and $Q^2 = -q^2$. The charm polarization function can further be expressed in terms of a dispersion relation

$$-\frac{d}{dQ^2}\Pi^{(c)}(Q^2) = \frac{1}{12\pi^2 Q_c^2}\int \frac{R_c(s)ds}{(s+Q^2)^2}, \quad (2)$$

where $Q_c = 2/3$ is the charm quark electric charge, and $R_c(s)$ is the imaginary part of the polarization function and is related to the cross section, σ_c as

$$R_c = \frac{3s\sigma_c}{4\pi\alpha^2}. \quad (3)$$

QCD sum rules states that the cross section, and thereby the polarization, can be formulated either from experimental data or theoretically from an operator product expansion (OPE). Since both of these should describe the same physics, the polarization function one obtains from either method should be the same. This leads to the construction of equations between the polarization function calculated using either the OPEs or the experimental data. These equations can be solved for various parameters of the OPEs.

As pointed out by SVZ, the OPE side of the sum rule becomes tractable when one considers a regime where asymptotic freedom allows one to use peturbative QCD. In general, this is valid for energies which satisfy $Q^2 + 4m_q^2 \gg \Lambda_{\rm QCD}^2$. For light quarks, this is only satisfied when $Q^2 \gg \Lambda_{\rm QCD}$. However, in the case of heavy quarks, such as charm, the relation holds even when $Q^2 = 0$. SVZ used this fact to construct QCD sum rules which are unique to heavy quark systems[1]. In the region of small Q^2, it is useful for comparisons to introduce the moments of the polarization function defined as,

$$\begin{aligned}\mathscr{M}_n &\equiv \frac{1}{12\pi^2 Q_c^2}\int \frac{R_c(s)ds}{s^{n+1}} \\ &= \frac{1}{n!}\left(-\frac{d}{dQ^2}\right)^n \Pi^{(c)}(Q^2)\bigg|_{Q^2=0}. \end{aligned} \quad (4)$$

One can then relate each moment between the OPE side and the experimental data rather than the entire polarization function. In the original work by SVZ [2, 3], using this method of comparison, they were able to calculate the heavy quark mass and show the need for nonperturbative corrections to have better agreement with the data.

Recently, the development of gauge/gravity dualities based upon the AdS/CFT correspondence [8–10] have led to holographic models which provide a new method of calculating the polarization function. Therefore it is natural to apply QCD sum rules as a way to understand, constrain, and evaluate possible holographic models. The OPE expansion has already been used for light quark holographic systems in order show that the AdS metric is sufficient to reproduce the leading large Q^2 behavior, [11,

---

*Electronic address: pmhohler@uic.edu

[1] Though in this note, we focus on the heavy quark sum rules at $Q^2 = 0$, heavy quark sum rules have been used at $Q^2 > 0$ based upon the initial work of Ref. [7]

12], and agreement with the OPE expansion has been a guiding principle in the construction of many light quark holographic models among which includes [13–17]. Yet this is the first time that these techniques will be applied to a holographic model with heavy quarks.

In the next section, the gauge/gravity dual models of charmonium [1, 5] are introduced. In Sec. III, the moments of the polarization function will be calculated from perturbative QCD as well as the holographic model [1]. This will be followed in Sec. IV by the results of the comparison of the moments between QCD and the holographic models, where the holographic models will take the role of the OPE side in the sum rules. Finally we will conclude, in Sec. V, with a discussion of the results.

II. CHARMONIUM MODEL FROM GAUGE/GRAVITY DUALITY

Key features relevant for the current discussions of holographic models of charmonium will be presented here. A more detailed exposition of these models can be found in Refs. [1] and [5]. The model of Ref. [1] will be referred to as the "shift and dip" model while the model of Ref. [5] will be referred to as the "rescaled ρ" model. The basic construction of the two models is similar, but the latter does not reproduce as many phenomenologically relevant features as the shift and dip model. The differences between the two models will be pointed out, and the two models will each be compared with the heavy quark QCD sum rules in the subsequent sections.

In the spirit of the holographic approach, it is assumed that the generating functional of the heavy quark vector current J^μ can be represented by the effective action obtained by integrating over a bulk 5D gauge field V_M (dual to the current) at a given fixed boundary value (equal to the source of the current). The action for the 5D gauge field is given by

$$S = -\frac{1}{4g_5^2} \int d^5x \sqrt{g}\, e^{-\Phi} V_{MN} V^{MN}, \qquad (5)$$

where g_5^2 is the 5D gauge coupling and $V_{MN} = \partial_M V_N - \partial_N V_M$. The 2-point current correlator is given by the linear response of the field V_M to an infinitesimal perturbation of its boundary condition.

The conformally flat representation for the 5D background metric g_{MN} with 4D Lorentz-isometry is chosen:

$$ds^2 \equiv g_{MN}\, dx^M dx^N = e^{2A(z)} \left[\eta_{\mu\nu} dx^\mu dx^\nu - dz^2 \right] \ , \ (6)$$

where $\eta_{\mu\nu} = \text{diag}(1,-1,-1,-1)$ is the Minkowski metric tensor. The effect of confinement is represented by the non-trivial background profile of the scalar field Φ in Eq. (5) in the same way as it is done in the soft-wall model with dilaton background in Ref. [18].

Following the rules of the holographic correspondence, the generating functional for correlation functions of the heavy-quark current can be calculated by evaluating the action at its extremum for given boundary conditions. The extremum is given by the solution of the equations of motion, which in $V_5 = 0$ gauge read:

$$\partial_z[e^{B(z)}\partial_z V] + q^2 e^{B(z)} V = 0 \ , \qquad (7)$$

where V is any of the three components $V_\perp$ of $V_\mu(z,q)$ transverse to 4-vector q^μ ($q^\perp = 0$) and

$$B = A - \Phi \ . \qquad (8)$$

Discrete values of $q^2 = m_k^2$, for which the Eq. (7) possesses a normalizable solution $V = v_k(z)$ satisfying the boundary condition $V|_{z=0} = 0$, correspond to the masses m_k of the charmonium states, $k = 1, 2, \ldots = J/\psi, \psi', \ldots$. We normalize such solutions as

$$\int_0^\infty dz\, e^{B(z)} v_k(z)^2 = 1 \ . \qquad (9)$$

The current-current correlator can be calculated according to the well-known prescription of Ref. [19, 20], by

$$G_R(q) = -\frac{1}{g_5^2} e^B V'(z,q)\Big|_{z=\epsilon} = -\frac{1}{g_5^2} \frac{V'(\epsilon,q)}{\epsilon}, \qquad (10)$$

where $\epsilon \to 0$ is an ultraviolet regulator and $V(z,q)$ is the non-normalizable solution of Eq. (7) with boundary conditions:

$$\begin{aligned} V(\epsilon, q) &= 1 \ ; \\ V(z,q) &\xrightarrow{z\to\infty} 0 \ . \end{aligned} \qquad (11)$$

The polarization function can then be determined by

$$\Pi^{(c)}(Q^2) = -\frac{1}{g_5^2 Q^2} e^B V'(z,q)\Big|_{z=\epsilon}, \qquad (12)$$

where $Q^2 = -q^2$. The ultraviolet behavior of the current-current correlator is required to be conformal, viz. $G_R(q) \sim q^2 \log(-q^2)$ as $q^2 \to -\infty$, which translates into:

$$e^{B(z)} \xrightarrow{z\to 0} z^{-1} \ , \qquad (13)$$

and matches that of QCD, which fixes [11, 12, 21]

$$g_5^2 = 12\pi^2/N_c \ . \qquad (14)$$

By performing a Liouville transformation,

$$\Psi = e^{B(z)/2} V \ , \qquad (15)$$

we can bring Eq. (7) to the canonical Schrödinger-like form

$$-d^2\Psi/dz^2 + U(z)\Psi = q^2\Psi \ , \qquad (16)$$

with the holographic potential given by

$$U(z) = \frac{B''(z)}{2} + \left(\frac{B'(z)}{2}\right)^2 \ . \qquad (17)$$

3

At this point the two holographic models differ. The rescaled ρ model chooses the metric warp factor to be $A(z) = -\log(z)$ and the dilaton profile to be $\Phi(z) = a^2 z^2$. This is precisely the form of the standard soft wall model [18]. This leads to a model of one parameter, viz. a, which is determined by fixing the mass of the J/ψ. Therefore the rescaled ρ model correctly reproduces the J/ψ mass (by construction), but the J/ψ decay constant and the ψ' mass and decay constant are all off by nearly 20%.

On the other hand, in the spirit of the bottom-up approach, the shift and dip model chooses the function B so as to satisfy the spectroscopic data associated with J/ψ and ψ'. It is assumed that such a background arises dynamically, but no attempt to model the corresponding dynamics is made. To this end, a holographic potential $U(z)$ is chosen:

$$U(z) = \frac{3}{4z^2}\,\theta(z_d - z) + \left((a^2 z)^2 + c^2\right)\theta(z - z_d) - \alpha\delta(z - z_d). \tag{18}$$

There are 4 parameters in this potential, which will be used to fit 4 experimental data points: the masses and the decay constants of J/ψ and ψ'. This potential may seem rather unusual, but it was chosen to reproduce the correct expected behavior at both small and large z as well as adding features, viz. the c^2 "shift" term and the delta function "dip" term, which facilitated the matching of the parameters to the physical constraints. The matched parameters were found to be

$$a = 0.970 \text{ GeV}, \ c = 2.781 \text{ GeV}, \\ \alpha = 1.876 \text{ GeV}, \ z_d^{-1} = 2.211 \text{ GeV}. \tag{19}$$

The potential in Eq. (18) can be, certainly, improved by applying further constraints. One goal of this paper is to determine how well this potential holds up to the additional constraints imposed by the heavy quark QCD sum rules.

Having established $U(z)$, the polarization function can be found by first solving Eq. (16) for the function $\Psi(z)$. Equation (17) can be solved for the function $B(z)$. Therefore the vector field can be calculated from $B(z)$ and $\Psi(z)$ using Eq. (15). Finally the polarization is calculated from Eq. (12) while its moments can be generated from Eq. (4).

III. CALCULATION OF MOMENTS

In this section, the moments will be calculated directly from the polarization function for the QCD OPE expansion and the shift and dip holographic model. The calculation of the polarization function using the rescaled ρ model is presented in Appendix A. The method to calculate the same moments from spectroscopic data will also be explored. A more general calculation of the moments for an arbitrary holographic model can be found in Appendix B.

A. OPE expansion

To calculate the moments for the QCD OPE expansion, we will concentrate on the leading unit operator term. Non-perturbative corrections, due primarily to the gluon condensate, can be included, but we will later show that this is unnecessary for our analysis here. This term can be calculated using peturbative QCD because of the heavy charm quark. At the 1-loop level, the imaginary part of the polarization function is given by,

$$R_c(s) = \frac{2}{3}v(3 - v^2)\,\theta(s - 4m_c^2), \tag{20}$$

where the heavy quark velocity is given by $v = (1 - 4m_c^2/s)^{1/2}$, and m_c is the charm quark mass. This expression can be used in the dispersion relation of Eq. (2) to calculate the polarization function, or it can be used in Eq. (4) to find it moments. This leads to the familiar result of [3] for the moments,

$$\mathscr{M}_n^{(0)} = \frac{3}{4\pi^2}\frac{2^n(n+1)(n-1)!}{(2n+3)!!}\frac{1}{(4m_c^2)^n}, \tag{21}$$

where superscript (0) refers to the fact that this is the leading order calculation. Note that charm quark mass is a free parameter of the OPE.

The leading α_s correction to the moments can also be calculated. With the inclusion of this correction the moments are given by,

$$\mathscr{M}_n = \mathscr{M}_n^{(0)} + \alpha_s \mathscr{M}_n^{(1)}, \tag{22}$$

where

$$\mathscr{M}_n^{(1)} = \mathscr{M}_n^{(0)}\left(\frac{4\sqrt{\pi}}{3}\frac{\Gamma(n+3/2)}{\Gamma(n+1)}\frac{1-(3n+3)^{-1}}{1-(2n+3)^{-1}} \right. \\ \left. -\frac{1}{2}\pi + \frac{3}{4\pi} - \frac{4n\log 2}{\pi} \right. \\ \left. -\frac{2}{3\sqrt{\pi}}\frac{2\pi^2-3}{4\pi}\frac{\Gamma(n+3/2)}{\Gamma(n+2)}\frac{1-2(3n+6)^{-1}}{1-(2n+3)^{-1}}\right). \tag{23}$$

B. Shift and dip model

In this section, the procedure discussed at the end of Sec. II will be used to determine the polarization function for the shift and dip model. The moments will not be explicitly calculated, but can be found from Eq. (4) using the polarization function. The results will be expressed in terms of the parameters a, c, α and z_d whose numerical values can be found in Eq. (19). First, one needs to calculate $B(z)$; this is done by solving Eq. (17) with the holographic potential giving by Eq. (18). This results in

$$e^{B(z)/2} = \begin{cases} \frac{1}{\sqrt{z}} + c_1\frac{z^{3/2}}{z_d^2} & z < z_d \\ c_2\,2^{\frac{a^2+c^2}{4a^2}}e^{-\frac{1}{2}a^2z^2}H_{\nu_1}(az) & z > z_d \end{cases}, \tag{24}$$

where $H_\nu(x)$ is the Hermite polynomial, $\nu_1 = -\frac{1}{2} - \frac{c^2}{2a^2}$, and c_1 and c_2 are integration constants given by,

$$
\begin{aligned}
c_1 &= \frac{\left(1 + 2\alpha z_d + 2a^2 z_d^2\right) H_{\nu_1}(az_d) - 2az_d H_{\nu_2}(az_d)}{\left(3 - 2\alpha z_d - 2a^2 z_d^2\right) H_{\nu_1}(az_d) + 2az_d H_{\nu_2}(az_d)}, \\
c_2 &= 2^{\frac{1}{2}\nu_1} e^{\frac{1}{2}a^2 z_d^2} \frac{1 + c_1}{\sqrt{z_d}\, H_{\nu_1}(az_d)},
\end{aligned}
\tag{25}
$$

where ν_1 is as before and $\nu_2 = \nu_1 + 1$. In order to determine the bulk vector field, $V(z,q)$, one needs to solve

Eq. (16) and use Eq. (15). This results in,

$$
V(z,q) = \begin{cases} \dfrac{c_3(Q^2)\, qz J_1(qz) - \frac{\pi}{2} qz\, Y_1(qz)}{1 + c_1 \left(\frac{z}{z_d}\right)^2} & z < z_d \\[3ex] c_4(Q^2) \dfrac{H_{\nu_{1q}}(az)}{H_{\nu_1}(az)} & z > z_d \end{cases}, \tag{26}
$$

where c_1 and c_2 are as before and $c_3(Q^2)$ and $c_4(Q^2)$ are given by,

$$
\begin{aligned}
c_3(Q^2) &= \frac{\pi}{2}\left(\frac{-2z_d q Y_0(qz_d) H_{\nu_{1q}}(az_d) + Y_1(qz_d)\left(\left(1 + 2\alpha z_d + 2a^2 z_d^2\right) H_{\nu_{1q}}(az_d) - 2az_d H_{\nu_{2q}}(az_d)\right)}{-2z_d q J_0(qz_d) H_{\nu_{1q}}(az_d) + J_1(qz_d)\left(\left(1 + 2\alpha z_d + 2a^2 z_d^2\right) H_{\nu_{1q}}(az_d) - 2az_d H_{\nu_{2q}}(az_d)\right)}\right) \\
c_4(Q^2) &= \frac{H_{\nu_1}(az_d)}{H_{\nu_{1q}}(az_d)} \frac{c_3(Q^2)\, qz_d J_1(qz_d) - \frac{\pi}{2}\, qz_d Y_1(qz_d)}{1 + c_1},
\end{aligned}
\tag{27}
$$

with $q^2 = -Q^2$, and $\nu_{1q} = \nu_1 + \frac{q^2}{2a^2}$, and $\nu_{2q} = \nu_{1q} + 1$. From this formula for the vector field, the polarization function can be found using Eq. (12),

$$
\Pi^{(c)}(Q^2) = \frac{-1}{g_5^2}\left(\gamma_{\mathrm{E}} + \log\left(\frac{iQ\epsilon}{2}\right) - c_3(Q^2) - \frac{2c_1}{Q^2 z_d^2}\right). \tag{28}
$$

One can show that for small Q^2, there are terms in $c_3(Q^2)$ which cancel both the c_1 term and the $\log(Q)$ term. This expression also has the standard $\log(\epsilon)$ divergence from the UV cutoff. This can be removed by renormalization such that $\Pi^{(c)}(0) = 0$. The moments can be generated from this expression using Eq. (4), however a simple analytic expression is not possible and therefore will not be presented here.

C. Spectroscopic data

The moments of the polarization function can also be determined directly from the spectroscopic data. If one assumes that the cross section can be constructed as a series of delta functions as is done in Refs. [3, 4], one for each charmonium state, R_c can be written as,

$$
\begin{aligned}
R_c(s) &= \frac{9\pi}{\alpha^2} \sum_k \delta(s - m_k^2) \frac{\Gamma_k^{ee}}{m_k} s \\
&= \frac{16\pi^2}{3} \sum_k \delta(s - m_k^2) \frac{f_k^2}{m_k^2} s,
\end{aligned}
\tag{29}
$$

where the sum is over all charmonium states with k labelling each state, Γ^{ee} is the electronic width, and f is the decay constant. The moments can then be calculated

by using this formula in Eq. (4),

$$
\mathcal{M}_n = \sum_k \frac{f_k^2}{m_k^{2n+2}}. \tag{30}
$$

Since the mass of the excited states tends to grow faster than its decay constant, the higher excited charmonium states are suppress for the higher moments. When considering the experimental spectrum, the spectrum exhibits a continuum of states above the $D\bar{D}$ threshold. SVZ approximated this continuum by choosing $R_c(s)$ to be

$$
R_c(s) = \frac{4}{3}\theta(s - 16\mathrm{GeV}^2), \tag{31}
$$

above the threshold. The contribution to the polarization function and the moments can as before be found by using Eq. (31) in Eqs. (2) and (4), respectively.

The necessary spectroscopic data, *viz.* the masses, m_k and decay constants, f_k, can either come from the physical experimental results [22], or it can be calculated from the spectrum of either holographic model. Unlike the experimental data, the holographic models contain only an infinite tower of zero width excited charmonium states with no continuum. Therefore, for good agreement between the moments of the holographic models and the experimental spetrum, one would hope that this tower of states can approximate the continuum of QCD.

The equivalence between the two methods to calculate the moments, *i.e.* from the polarization function or from the spectrum, is due to equivalent ways of expressing the polarization function. One tends to use the method which is easier to calculate with. In this paper, discussions will highlight the method using the spectroscopic data since it is more natural to interpret the results

in the language of this method, though both techniques yield the same numerical results.

IV. RESULTS

To assess the consistency of the holographic model of charmonium with the heavy quark QCD sum rules, we will examine the moments of the polarization function qualitatively and quantitatively. The moments calculated from the holographic model will be compared to those calculated from the experimental spectroscopic data and from perturbative QCD. In order to provide a baseline for the results of the shift and dip model, the results using the rescaled ρ model will also be presented.

To begin, we will use the techniques of SVZ to analyze the moments of the polarization function. The polarization function's moments will be calculated for each holographic model using each model's spectral data as detailed in Sec. III C. For both holographic models, a sufficient number of excited states were considered[2]. The moments of the polarization function is also calculated from the first 2 experimentally known charmonium states and a contribution for the continuum as done in [4].

The ratio of the moments of the polarization function between each holographic model and the experimental data are constructed and presented in Table I with superscript A referring to the shift and dip model and superscript B referring to the rescaled ρ model. The results indicate that the shift and dip model is consistent with QCD at worst at the 20% level with even better agreement for the higher moments. This is quite reasonable considering that there should be $1/N_c$ corrections to the holographic model.

Moment n	$\mathscr{M}_n^A/\mathscr{M}_n^{\text{Expt}}$	$\mathscr{M}_n^B/\mathscr{M}_n^{\text{Expt}}$
1	0.79	0.54
2	0.91	0.57
3	0.96	0.59
4	0.98	0.60
5	0.99	0.61

TABLE I: Ratio of the polarization function moments calculated using either holographic model to the moment calculated using QCD. The label A refers to the shift and dip model while the label B refers to the rescaled ρ model.

The better agreement between the shift and dip model and QCD for the higher moments can be understood by the fact that the higher excited states are suppressed for these moments as discussed in Ref. [3, 4]. Therefore the largest contribution for both the holographic model and

QCD comes from the J/ψ and ψ' states which are identical in both cases by construction. For example the J/ψ and ψ' contribute only 75% to the first moment in the shift and dip model while this climbs to 99% for the fifth moment. Therefore the larger discrepancy seen in the first moment is an indication that the tower of excited states in the holographic model only marginally approximates the QCD continuum.

The rescaled ρ model also has improved agreement with QCD for the higher moments because of the increase in the contribution of the J/ψ to these moments. However, the differences seen between the shift and dip model and the rescaled ρ model in Table I can be attributed to fact that the rescaled ρ model does not accurately reproduce the ψ' state.

Another useful way to compare the holographic model to the QCD OPE and the experimental data is to look at the ratio of consecutive moments; defined as

$$r_n = \frac{\mathscr{M}_n}{\mathscr{M}_{n-1}}. \qquad (32)$$

Figure 1 plots the results for r_n from perturbative QCD, the experimental data, and both holographic models. The moments of the polarization function for the experimental data and the holographic models are calculated as described above. The polarization function's moments from perturbative QCD are found from Eq. (23) with $m_Q = 1.21\text{GeV}$. The charm quark mass was found by equating the first moment calculated from the QCD OPE and the first moment calculated from the experimental data and solving for the heavy quark mass. The points at $n = 1$ correspond to the value of the first moment multiplied by the factor $(4\pi/3)^2$, as is done by SVZ [3]. Again the discrepancy seen between these values is indicative that the tower of excited states of the shift and dip model does not reproduce the experimental continuum well. One can see that for the highest moments the holographic models agree significantly well with the experimental data. Again this is not that surprising since the highest moments have a larger contribution from the J/ψ state. The discrepancy seen between the shift and dip model and the rescaled ρ model at the highest moments is because the rescaled ρ model only reproduces the J/ψ mass and not the decay constant. Furthermore, the perturbative QCD calculation with only the leading α_s corrections, does not agree very well with the experimental data for the higher moments. SVZ showed, [3], that this discrepancy can be resolved by including the effects of the gluon condensate. The good agreement between the holographic models would imply that they correctly capture the non-perturbative physics of the charm system.

The quantitative results from the moments can be summarized graphically by plotting the polarization function directly. Figure 2 depicts the polarization function as a function of Q^2 for small Q^2 calculated using the experimental spectroscopic data (solid curve), the shift and dip model (dashed curve), and the rescaled ρ model

---

[2] For the shift and dip model, 400 states were used, while for the rescaled ρ model, one can analytically calculate for infinite number of states.
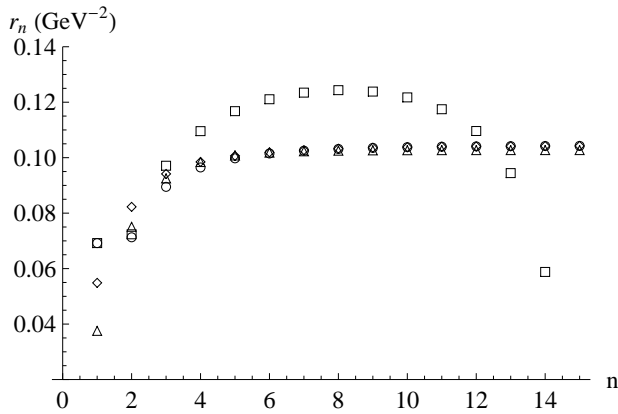
FIG. 1: Ratio of consecutive moments calculated from perturbative QCD (squares), spectroscopic data (circles), the shift and dip model (diamonds), and the rescaled ρ model (triangles).

V. DISCUSSION

In this paper, we have considered a holographic model of charmonium and analyzed it in the context of heavy quark QCD sum rules. We have illustrated how to calculate the moments of the polarization function for this model. The moments have then been used to compare the holographic models to the results obtained from the QCD OPE expansion and the experimental spectroscopic data.

The results have shown that the holographic model of charmonium presented in Ref. [1] agrees very well, more than 80% for the first moment and reaching above 90% for the higher moments, with heavy quark QCD sum rules. This was shown via graphical means and by directly examining the moments of the polarization function.

This has been the first time that heavy quark QCD sum rules have been applied to a holographic model. It is not obvious *a priori* that for the heavy quark sector the agreement between the holographic model and QCD for $Q^2 < 0$ translates into agreement between the holographic model and QCD for $Q^2 > 0$. Nevertheless, within reasonable uncertainties, this is exactly what we have demonstrated here. The results of the shift and dip model have been compared to another holographic model as a baseline comparison. This has illustrated that the added phenomenological constraints imposed in constructing the shift and dip model simultaneously improves the agreement with the QCD sum rules. Clearly this agreement is enhanced by the fact that the moments have a dominant contribution from the J/ψ and ψ' states. However, the agreement, in particular for the first moment when the contributions from J/ψ and ψ' to the moment are not as significant, is non-trivial.

As one progresses to future holographic models of heavy quark systems, it will be important to understand how these systems scale with the quark mass. In this way, one may be able to relate aspects of the holographic models found in heavy quark systems back to their light mass cousins. Moreover, most of the discrepancies between the shift and dip model and the QCD sum rules seem to stem from discrepancies associated with the first moment. Any future attempts to improve the agreement must address this issue. Since each moment from the shift and dip model is smaller than from the QCD OPE, to improve agreement one must either increase the decay constants of the excited states or decrease their masses. As discussed in the construction of the shift and dip model in [1], these adjustments may be accomplished by changing the holographic potential, Eq. (18), by further increasing the region of attraction, both in strength and width, in the area of $z \sim m_q^{-1}$, or by possibly softening the softwall, respectively. Obviously, any future changes would still need to be consistent with the spectroscopic data of the first two charmonium states.

In conclusion, we have demonstrated that the holographic shift and dip model is consistent in a non-trivial

(dotted curve). Each function has been renormalized so that $\Pi^{(c)}(Q^2 = 0) = 0$. The curve from the experimental data is calculated from Eq. (2) using Eqs. (29) and (31). The shift and dip curve is a plot of Eq. (28) with the parameters chosen from Eq. (19) while the rescaled ρ curve plots Eq. (A3). Note, though not shown, the polarization function determined from the perturbative QCD calculation would lie directly on top of the experimental curve. From the figure, one can clearly see that the charmonium model with a shift and a dip has better agreement with experimental data as compared with the rescaled ρ model. The polarization function calculated from the shift and the dip model is in modest agreement with the QCD calculation (within 21%) for $Q^2 < 1\text{GeV}^2$, but remains within 26% agreement to $Q^2 = 10\text{GeV}^2$. This uncertainty is associated with the discrepancy of the first moment seen in Table I.
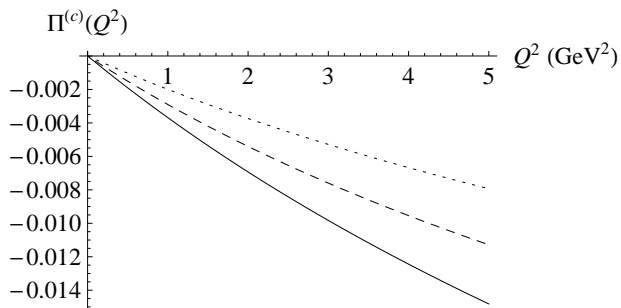

FIG. 2: Polorization function $\Pi^{(c)}$ at small Q^2 for the perturbative QCD calculation to order α_s (solid line), the shift and dip model (dashed line), and the rescaled ρ model (dotted line). All functions have been renormalized so $\Pi^{(c)}(0) = 0$.

manner with the QCD sum rules at zero temperature.

Appendix A: Rescaled ρ model

For the rescaled ρ model, the moments can be calculated using the procedure outlined at the end of Sec. II. However one does not need to solve any equations for the function $B(z)$ since it is provided from the soft-wall model. This function can be expressed as

$$e^{B(z)} = \frac{1}{z} e^{-a^2 z^2}, \qquad (A1)$$

where a is a parameter of the model which is determined by requiring the model reproduce the mass of J/ψ correctly. Numerically it is $a = 1.56\text{GeV}$. From this expression for $B(z)$, one can determine $V(z)$ subject to the boundary conditions as,

$$V(z,q) = \Gamma\left(1 - \frac{q^2}{4a^2}\right) U\left(-\frac{q^2}{4a^2}, 0, a^2 z^2\right), \qquad (A2)$$

where $U(a,b,x)$ is the Tricomi confluent hypergeometric function. This expression for $V(z,q)$ can then be used in Eq. (12) to determine the polarization function for this model. This results in

$$\Pi^{(c)}(Q^2) = -\frac{1}{2g_5^2}\left[\gamma_E + \psi\left(1 + \frac{Q^2}{4a^2}\right)\right], \qquad (A3)$$

where $Q^2 = -q^2$, γ_E is the Euler gamma, and $\psi(x)$ is the Polygamma (or Digamma) function. This function has already been renormalized so $\Pi^{(c)}(0) = 0$. The moments of the polarization function can be easily found using Eq. (4) resulting in,

$$\mathcal{M}_n = \frac{1}{2g_5^2} \frac{1}{(4a^2)^n} \zeta(n+1), \qquad (A4)$$

where $\zeta(x)$ is the Zeta function.

Appendix B: Determining the moments of the polarization function for a holographic model

In Sec. III, the moments of the polarization function were calculated for a particular holographic model of charmonium. In each case, one could solve the necessary differential equation analytically, so an analytic expression for the polarization function was possible. However, for an arbitrary holographic model with a vector field

this may not be the case. In this appendix, we will calculate the moments for this arbitrary holographic model in terms of integral recursive relations. These can be used when an analytic solution is possible, but will most likely be more useful when one is required to rely on numerics.

To construct the moments, we will once again use the same procedure that was outlined at the end of Sec. II. However, since we wish to consider a large class of theories, we will leave the function $B(z)$ unspecified. Therefore, we begin with the equation of motion for the vector field of Eq. (7),

$$V''(z,Q^2) + B'(z)V'(z,Q^2) - Q^2 V(z,Q^2) = 0, \quad (B1)$$

where $q^2 = -Q^2$. As before, this equation is subject to the boundary conditions of Eq. (11). Since we are interested in the polarization function at small Q^2, we can explore Eq. (B1) in the same limit. Therefore we will assume that $V(z,Q^2)$ can be expanded in a Taylor series of Q^2, namely,

$$V(z,Q^2) = \sum_{n=0} \left(-Q^2\right)^n V_n(z). \qquad (B2)$$

The functions $V_n(z)$ correspond to the coefficients in the Taylor series. Note these should not be confused with the eigenmodes of the differential equation. By inserting Eq. (B2) into Eq. (B1) and equating powers of Q^2, one arrives at a difference equation for the functions $V_n(z)$.

$$V_n'' + B'V_n' = -V_{n-1}, \qquad (B3)$$

which can be solved by iterative means.

The 0th order expression,

$$V_0'' + B'V_0' = 0, \qquad (B4)$$

can be easily solved,

$$V_0(z) = b_1 + b_2 \int_0^z e^{-B(z')} dz'. \qquad (B5)$$

The integration constants, b_1 and b_2, can be determined from the boundary conditions resulting in $V_0(z) = 1$[3]. For larger values of n, the equation can be solved by a Green's function technique. Therefore the solutions can be written as

$$V_n(z) = \int_\epsilon^\infty dz' G(z,z') V_{n-1}(z'), \qquad (B6)$$

where $G(z,z')$ is defined to satisfy the differential equation

$$\frac{\partial^2 G(z,z')}{\partial z^2} + B'(z)\frac{\partial G(z,z')}{\partial z} = -\delta(z - z'). \qquad (B7)$$

---

[3] Though this expression does not explicitly satisfy the boundary condition for $V(z,Q^2)$ at infinity, we have assumed that $V_n(z)$ should at least be finite in this limit. The boundary condition for $V(z,Q^2)$ would then be satisfied once the infinite sum in Eq. (B2) is performed.

8

To be consistent with the boundary conditions on $V(z,Q^2)$ and the expression for $V_0(z)$, $G(z,z')$ must satisfy the boundary conditions $G(\epsilon,z') = 0$ and $G(z,z')$ is finite as $z \to \infty$.

Equation (B7) can be solved to the left and to the right of delta function as

$$G(z,z') = \begin{cases} b_3 + b_4 \int_\epsilon^z e^{-B(z'')}dz'' & z < z' \\ b_5 + b_6 \int_{z'}^z e^{-B(z'')}dz'' & z > z' \end{cases}. \quad (B8)$$

The integration constants can be determined from the boundary conditions and the matching conditions at the delta function resulting in the Green's function to be expressed as,

$$G(z,z') = e^{B(z')} \int_\epsilon^{z_<} e^{-B(z'')}dz'', \quad (B9)$$

where $z_<$ is the smaller of z and z'. It is useful to note the derivative of the Green's function with respect to z,

$$\frac{\partial G(z,z')}{\partial z} = \theta(z'-z)\left(e^{B(z')-B(z)}\right), \quad (B10)$$

where θ is the unit step function.

Having determined the appropriate Green's function, $V_n(z)$ for $n \geq 1$ can be generated from Eq. (B6), in particular $V_1(z)$ can be written as,

$$\begin{aligned} V_1 &= \int_\epsilon^\infty G(z,z')V_0(z')dz' \\ &= \int_\epsilon^z \left(e^{B(z')}\int_\epsilon^{z'} e^{-B(z'')}dz''\right)dz' \\ &\quad + \int_z^\infty \left(e^{B(z')}\int_\epsilon^z e^{-B(z'')}dz''\right)dz' \\ &= \int_\epsilon^z dz' e^{-B(z')}\int_{z'}^\infty e^{B(z'')}dz''. \end{aligned} \quad (B11)$$

The notation here can be compactified some by defining the functions $\alpha(z)$ and $\beta(z)$ as

$$\begin{aligned} \alpha(z) &\equiv \int_\epsilon^z e^{-B(z')}dz', \\ \beta(z) &\equiv \int_z^\infty e^{B(z')}dz'. \end{aligned} \quad (B12)$$

Using this notation the Eq. (B9) can be written as

$$G(z,z') = \begin{cases} -\beta'(z')\alpha(z) & z < z' \\ -\beta'(z')\alpha(z') & z > z' \end{cases}, \quad (B13)$$

and $V_1(z)$ as

$$V_1(z) = \int_\epsilon^z \beta(z')\alpha'(z')dz'. \quad (B14)$$

Having determined the functions V_n in terms of the Green's function and V_{n-1}, let us turn our attention to

the polarization function and its moments. As before, Eq. (12) relates the polarization function to the vector field. Using the expansion in Q^2 for $V(z,Q^2)$ in Eq. (B2), we can we can expand $\Pi^{(c)}$ in powers of Q^2,

$$\Pi^{(c)} = \frac{1}{g_5^2}\sum_{n=-1}(-Q^2)^n \left(e^{B(z)}V'_{n+1}(z)\right)_{z\to\epsilon}. \quad (B15)$$

One may worry since this expansion seems to have a $(Q^2)^{-1}$ term. However upon further inspection, the coefficient of this term is $e^{B(z)}V'_0(z)\big|_{z\to\epsilon}$, and with the previous assessment that $V_0(z) = 1$, this term is exactly 0. The expansion also contains a term constant in Q^2. This term can always be eliminated by renormalizing the polarization function such that $\Pi^{(c)}(0) = 0$.

The moments can be calculated in the normal manner from Eq. (4) and yield,

$$\begin{aligned} \mathscr{M}_n &= \frac{1}{g_5^2}\left(e^{B(z)}V'_{n+1}(z)\right)_{z\to\epsilon} \\ &= \frac{1}{g_5^2}e^{B(\epsilon)}\int_\epsilon^\infty G'(\epsilon,z')V_n(z')dz' \\ &= \frac{1}{g_5^2}\int_\epsilon^\infty e^{B(z')}V_n(z')dz', \end{aligned} \quad (B16)$$

where Eqs. (B6) and (B10) are used for lines two and three respectively. The moment can be expressed using the compact notation as

$$\mathscr{M}_n = \frac{1}{g_5^2}\int_\epsilon^\infty \beta(z)V'_n(z)dz. \quad (B17)$$

The first moment can be explicitly calculated as,

$$\begin{aligned} \mathscr{M}_1 &= \frac{1}{g_5^2}\int_\epsilon^\infty e^{B(z)}V_1(z)dz \\ &= \frac{1}{g_5^2}\int_\epsilon^\infty e^{B(z)}\left[\int_\epsilon^z \left(e^{-B(z')}\int_{z'}^\infty e^{B(z'')}dz''\right)dz'\right]dz \\ &= \frac{1}{g_5^2}\int_\epsilon^\infty dz\, e^{-B(z)}\left(\int_z^\infty e^{B(z')}dz'\right)^2, \end{aligned} \quad (B18)$$

or in the compact notation,

$$\mathscr{M}_1 = \frac{1}{g_5^2}\int_\epsilon^\infty \beta(z)^2\alpha'(z)dz. \quad (B19)$$

All higher moments can then be found by iteratively solving Eq. (B3) for $V_n(z)$ and using it in Eq. (B16). One can easily see that, for this class of holographic models, $\mathscr{M}_n$ is positive for all values of n.

[1] H. R. Grigoryan, P. M. Hohler and M. A. Stephanov, arXiv:1003.1138 [hep-ph].

[2] M. A. Shifman, A. I. Vainshtein and V. I. Zakharov, Nucl. Phys. B **147**, 385 (1979).

[3] M. A. Shifman, A. I. Vainshtein and V. I. Zakharov, Nucl. Phys. B **147**, 448 (1979).

[4] V. A. Novikov, L. B. Okun, M. A. Shifman, A. I. Vainshtein, M. B. Voloshin and V. I. Zakharov, Phys. Rept. **41**, 1 (1978).

[5] M. Fujita, K. Fukushima, T. Misumi and M. Murata, Phys. Rev. D **80**, 035001 (2009).

[6] M. Fujita, K. Fukushima, T. Kikuchi, T. Misumi and M. Murata, arXiv:0911.2298 [hep-ph].

[7] L. J. Reinders, H. Rubinstein and S. Yazaki, Phys. Rept. **127**, 1 (1985).

[8] J. M. Maldacena, Adv. Theor. Math. Phys. **2**, 231 (1998) [Int. J. Theor. Phys. **38**, 1113 (1999)];

[9] S. S. Gubser, I. R. Klebanov and A. M. Polyakov, Phys. Lett. B **428**, 105 (1998);

[10] E. Witten, Adv. Theor. Math. Phys. **2**, 253 (1998).

[11] J. Erlich, E. Katz, D. T. Son and M. A. Stephanov, Phys. Rev. Lett. **95**, 261602 (2005).

[12] L. Da Rold and A. Pomarol, Nucl. Phys. B **721**, 79 (2005)

[arXiv:hep-ph/0501218].

[13] J. Hirn, N. Rius and V. Sanz, Phys. Rev. D **73**, 085005 (2006) [arXiv:hep-ph/0512240].

[14] C. Csaki and M. Reece, JHEP **0705**, 062 (2007) [arXiv:hep-ph/0608266].

[15] S. S. Afonin, Phys. Lett. B **678**, 477 (2009) [arXiv:0902.3959 [hep-ph]].

[16] L. Cappiello and G. D'Ambrosio, arXiv:0912.3721 [hep-ph].

[17] T. Hambye, B. Hassanain, J. March-Russell and M. Schvellinger, Phys. Rev. D **76**, 125017 (2007) [arXiv:hep-ph/0612010].

[18] A. Karch, E. Katz, D. T. Son and M. A. Stephanov, Phys. Rev. D **74**, 015005 (2006).

[19] D. T. Son and A. O. Starinets, JHEP **0209**, 042 (2002).

[20] C. P. Herzog and D. T. Son, JHEP **0303**, 046 (2003) [arXiv:hep-th/0212072].

[21] D. T. Son and M. A. Stephanov, Phys. Rev. D **69**, 065020 (2004) [arXiv:hep-ph/0304182].

[22] C. Amsler et al. (Particle Data Group), Physics Letters B667, 1 (2008) and 2009 partial update for the 2010 edition.